

Synthesis of tailored bimodal mesoporous materials with independent control of the dual pore size distribution

Jihong Sun, Zhiping Shan, Thomas Maschmeyer, Jacob A. Moulijn and Marc-Olivier Coppens*

Department of Chemical Technology, Delft University of Technology, Julianalaan 136 2628 BL, Delft, The Netherlands. E-mail: M.O.Coppens@tnw.tudelft.nl

Received (in Cambridge, UK) 1st October 2001, Accepted 6th November 2001

First published as an Advance Article on the web 21st November 2001

A new synthesis method is presented to prepare multi-structured porous materials through a fully chemical route that allows control of the smaller and larger mesopore sizes independently.

A well-defined pore size distribution at various scales is desirable for a variety of applications.¹ Experiments and simulations have shown that a hierarchical combination of independently controlled, well-connected smaller and larger mesopores² reduces transport limitations in catalysis, resulting in higher activities and better controlled selectivities.³

Since the first reported syntheses of MCM-41, there has been intense research activity in designing and synthesizing structured mesoporous solids with controlled pore sizes.⁴ Recently, using a variety of techniques, *physical* templating methods were proposed to create large meso- or macropores.⁵ However, scale-up of these approaches may not be easy or cheap, prompting for the development of alternative *chemical* templating methods by which larger mesopores (≥ 10 nm) could be produced in a controlled way.

Here, we present such a method by means of which particles of a primary mesoporous material, *e.g.* MCM-41, are cross-linked using triblock copolymer assemblies as templating agents to form a material with a secondary bimodal pore distribution. By varying the synthesis conditions in the second step, it is possible to synthesize a broad class of such hierarchically structured silicas (Table 1).

In the first step tetraethylorthosilicate, the template cetyltrimethylammonium bromide (CTAB), water and ammonia were mixed at room temperature in a ratio of 1:0.2:160:1.5. This 'primary product' was filtered off and repeatedly washed with distilled water. After drying and calcination, the structure of the 'primary product' was confirmed by XRD (Fig. 1) and nitrogen adsorption, as MCM-41.⁶ Its isotherm (sample 1) is consistent with a narrow pore size distribution around 2.6 nm (Fig. 2), as expected for MCM-41.[†] In the second step, prior to drying, part of the filtered 'primary product' was immersed in a

basic (pH ~ 10) 5 wt% solution of a tri-block copolymer surfactant (*e.g.*, P-123) in a solvent (*e.g.*, ethanol). After aging the gel for 2 d in an autoclave at 100 °C, the 'secondary product' was filtered off, repeatedly washed with distilled water, dried at 120 °C for 3 h and calcined at 500 °C for 6 h in air. The formation of novel structures within the secondary product can be deduced from the N₂ adsorption-desorption isotherms of the calcined samples.

The isotherms of all secondary products (samples 2–8), exhibit two inflections (Fig. 2). The first of these (a flat hysteresis loop at $0.4 < P/P_0 < 0.55$) is shifted to a higher relative pressure compared to that of the primary product, and corresponds to a mean pore size of around 3.0–3.3 nm. Meanwhile, the XRD patterns of the secondary products show that the order of the pores has decreased somewhat, while the (100) peak is slightly shifted to lower angles (corresponding to a *d*-spacing of ~ 4.2 nm), due to the small primary pore size increase (Fig. 1). This results from solvent penetration in the second step into the hydrophobic core of the liquid crystalline template formed by CTAB.⁷ The second inflection (a type IV-A hysteresis loop at $0.8 < P/P_0 < 0.98$) indicates the presence of a significant amount of secondary mesopores, with a synthesis dependent pore size distribution at scales > 10 nm (Fig. 2 and

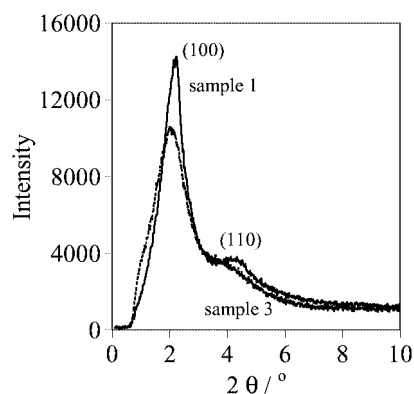


Fig. 1 XRD patterns of samples 1 and 3.

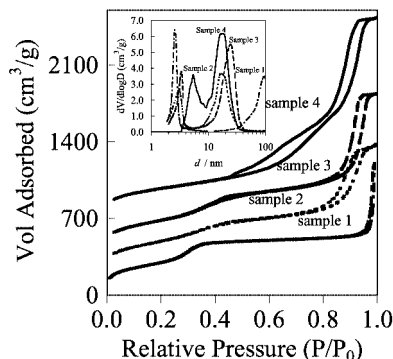


Fig. 2 Nitrogen adsorption-desorption isotherms of the samples (inset: corresponding pore size distributions). Subsequent isotherms are offset by 200 cm³ g⁻¹.

Table 1 Texture properties of the samples

Sample	SF ^a	Solvent	<i>d</i> ^b /nm		PV ^c /cm ³ g ⁻¹	SA ^d /m ² g ⁻¹
			Prim.	Sec.		
1			2.6		0.7	1100
2		Ethanol	3.1	16	1.8	1070
3	P-123 ^e	Ethanol	3.3	25	2.6	960
4	P-123	Benzene	5.4	16	2.8	980
5	P-123	Water	3.2	54	2.8	950
6	L-61 ^f	Ethanol	3.3	36	3.5	990
7	P-64 ^g	Ethanol	3.0	25	2.9	990
8	F-68 ^h	Ethanol	3.1	22	2.4	1020

^a Surfactant. ^b Mean pore diameter. Calculated on the basis of the BJH model for the desorption branch of nitrogen adsorption isotherms. ^c Pore volume. ^d Surface area. ^e HO(CH₂CH₂O)₂₀(CH₂CH₂CH₂O)₇₀(CH₂CH₂O)₂₀H. ^f HO(CH₂CH₂O)₂(CH₂CH₂CH₂O)₃₁(CH₂CH₂O)₂H. ^g HO(CH₂CH₂O)₁₃(CH₂CH₂CH₂O)₃₀(CH₂CH₂O)₁₃H. ^h HO(CH₂CH₂O)₇₆(CH₂CH₂CH₂O)₂₉(CH₂CH₂O)₇₆H.

Table 1). The shape of this hysteresis loop is quite different in its width from the secondary loop of the primary product in the same region and suggests tubular pores instead of interparticle, textural mesoporosity.⁸ At the low surfactant concentrations used here, the micelles do not form a liquid crystal phase, but disordered spherical to flexible rod- or worm-like micelles.⁹

During the initial stage of the secondary product synthesis, the primary MCM-41 gel particles are still soft and deformable; surface silanol groups exposed to the micelles form hydrogen bonds with their hydrophilic heads, while silanol groups of adjoining particles condense around the micelles at the higher temperatures in the autoclave. This view is supported by an examination of ²⁹Si magic-angle spinning nuclear magnetic resonance (MAS-NMR) spectra of the secondary materials which show for, e.g., sample 3, three broad peaks at 91 (Q²), 101 (Q³) and 109 ppm (Q⁴). The ratio of the peak areas is Q²:Q³:Q⁴ = 0.03:0.34:1, whereas for the primary material (sample 1) it is 0.2:0.46:1. This suggests that the secondary materials are somewhat more condensed as would be expected as a result of covalent cross-linking.¹⁰

The conditions during the first step are kept constant, resulting in primary gel particles that are reproducibly within the same size range ~20 nm and the pore size distribution of which centers around 3.1 nm. Mainly by using different solvent and/or surfactant compositions during the second synthesis step, the pore size distribution of the secondary material can be controlled without appreciably modifying the pore size distribution of the primary product.

Two experiments show the role P-123 plays during the formation of secondary product. In a "blank" experiment (not using any micelle-forming P-123 in the second synthesis step, sample 2) a secondary product was obtained, the isotherm of which is consistent with a pore size of 16 nm with a 10 nm width, indicating textural mesoporosity. In a second experiment, using non-polar benzene instead of ethanol as solvent with 5 wt% P-123 (sample 4), the peak of the primary product pore size distribution shifts from 3 to 5.4 nm, because benzene is able to considerably swell CTAB aggregates/micelles located inside the primary product pores. The average secondary pore size is the same as that when no P-123 is used (*i.e.* 16 nm with a width of 10 nm). Benzene, being a better organic solvent than ethanol, dissolves P-123 completely without leading to micelle formation,¹¹ thus resulting in the same secondary pore size as obtained in the absence of copolymer (sample 2). Therefore, only in the presence of P-123 and under conditions where it can form micelles do we observe mesopores larger than 20 nm (*viz.* Table 1) of tubular type. The secondary pore size of sample 1 (> 100 nm) is even larger due to textural interparticle meso/macroporosity.

These data are consistent with our postulate that the two pore systems are formed in independent processes. The mechanism for the formation of MCM-41 is well established,^{4a,6} but for the generation of the larger mesopores in the secondary product, it is suggested that in ethanol the surfactants form micelles around which the soft particles of the primary product cross-link by condensation of the surface hydroxy groups of adjoining particles. This is schematically shown in Fig. 3. The size of the micelles, and, therefore, of the so-generated larger secondary pores, depends on the synthesis conditions [*e.g.*, surfactant composition (compare samples 6, 7 and 8), solvent polarity (compare samples 4, 3 and 5), and amount of surfactant]. A similar route to fabricate nanotubes has recently been reported.¹²

Transmission electron microscopy (TEM) images are also consistent with a bimodal pore system, showing regions of less ordered, worm-like, small mesopore channels with a diameter of 3 nm, as well as tubular, rounded, large mesopores with a diameter around 40 nm for, *e.g.*, sample 6, consistent with the

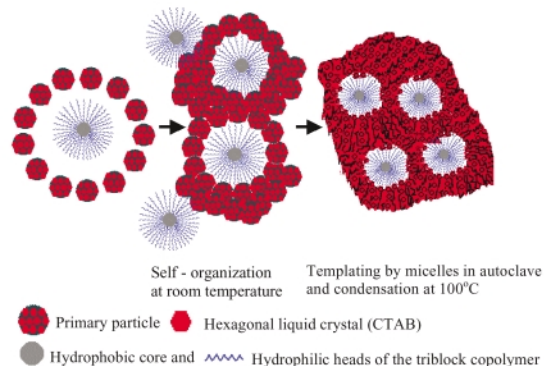


Fig. 3 Schematic representation of bimodal pore formation in the second step.

N₂ adsorption results. It should be noted that the contrast obtainable for amorphous siliceous materials is always inferior to that of ordered materials. Scanning electron microscopy (SEM) images show a smoother morphology for the secondary product compared to the particulate morphology of the primary product.

The method presented here provides a general means to synthesize multi-structured materials with a controlled pore structure over a range of scales. An efficient, hierarchical "road network" can, thus, be designed in a purely chemical way, leading to the desirable structure for a particular application.

We thank Dr P. J. Kooyman for the TEM and P. Boeser for measurement of the adsorption isotherms.

Notes and references

† The typical sharp increase at high pressure is due to inter-particle macroporosity. Also, the XRD pattern is typical for a hexagonally ordered MCM-41, with a *d*-spacing of 3.9 nm for the (100) peak.

- P. D. Yang, T. Deng, D. Y. Zhao, J. L. Feng, D. Pine, B. F. Chmelka, G. M. Whitesides and G. D. Stucky, *Science*, 1998, **282**, 2244.
- T. R. Pauly, Y. Liu, T. J. Pinnavaia, S. J. L. Billinge and T. P. Rieker, *J. Am. Chem. Soc.*, 1999, **121**, 8835; S. T. Wong, H. P. Lin and C. Y. Mou, *Appl. Catal., A: Gen.*, 2000, **198**, 103.
- M.-O. Coppens and G. F. Froment, *Fractals*, 1997, **5**, 493.
- (a) C. T. Kresge, M. E. Leonowicz, W. J. Roth, J. C. Vartuli and J. S. Beck, *Nature*, 1992, **359**, 710; (b) A. Corma, Q. Kan, M. T. Navarro, J. Perez-Pariente and F. Rey, *Chem. Mater.*, 1997, **9**, 2123; (c) D. Khushalani, A. Kuperman, G. A. Ozin, K. Tanaka, J. Garces, M. M. Olken and N. Coombs, *Adv. Mater.*, 1995, **7**, 842.
- B. T. Holland, C. F. Blanford and A. Stein, *Science*, 1998, **281**, 538; A. Imhof and D. J. Pine, *Nature*, 1997, **389**, 948; O. D. Velev, T. A. Jede, R. F. Lobo and A. M. Lenhoff, *Nature*, 1997, **389**, 447; L. M. Huang, Z. B. Wang, J. B. Sun, L. Miao, Q. Z. Li, Y. S. Yan and D. Y. Zhao, *J. Am. Chem. Soc.*, 2000, **122**, 3530; C. J. H. Jacobsen, C. Madsen, J. Houzvicka, I. Schmidt and A. Carlsson, *J. Am. Chem. Soc.*, 2000, **122**, 7116.
- J. S. Beck, J. C. Vartuli, W. J. Roth, M. E. Leonowicz, C. T. Kresge, K. D. Schmitt, C. T.-W. Chu, D. H. Olson, E. W. Sheppard, S. B. McCullen, J. B. Higgins and J. L. Schlenker, *J. Am. Chem. Soc.*, 1992, **114**, 10834.
- J. H. Sun, J. A. Moulijn, J. C. Jansen, Th. Maschmeyer and M.-O. Coppens, *Adv. Mater.*, 2001, **13**, 327.
- S. J. Gregg and K. S. W. Sing, *Adsorption, Surface Area and Porosity*, Academic Press, London, 2nd edn., 1982.
- S. A. Bagshaw, E. Prouzet and T. J. Pinnavaia, *Science*, 1995, **269**, 1242; P. Alexandridis and K. Andersson, *J. Phys. Chem. B*, 1997, **101**, 8103; J. P. Zhao, S. G. Wang, Y. J. Gong, D. Wu and Y. H. Sun, *Chem. J. Chin. Univ.*, 2000, **21**, 1797.
- L. L. Hench and J. K. West, *Chem. Rev.*, 1990, **90**, 33.
- P. Alexandridis and L. Yang, *Macromolecules*, 2000, **33**, 5574.
- J. Ruez, R. Barjovanu, J. A. Massey, M. A. Winnik and I. Manners, *Angew. Chem., Int. Ed.*, 2000, **39**, 3862.